DESIGN AND FABRICATION OF A COMPACT QUAD-BAND BANDPASS FILTER USING TWO DIFFERENT PARALLEL POSITIONED RESONATORS

C.-F. Yang

Department of Chemical and Materials Engineering
National University of Kaohsiung, Kaohsiung, Taiwan

Y.-C. Chen and C.-Y. Kung

Department of Electrical Engineering
National Sun Yat-sen University, Kaohsiung, Taiwan

J.-J. Lin and T.-P. Sun

Department of Applied Materials and Optoeletronic Engineering
National Chi Nan University, Taiwan

Abstract—A novel microstrip quad-band bandpass filter was designed and fabricated on an Al_2O_3 ceramic substrate of 1 mm thick. Two different types of open-loop resonator — a winding line-shaped resonator (WLR) and a stepped impedance resonator (SIR) — were positioned in parallel at the two sides of input/output microstrip lines that had the same coupling lengths and coupling gap widths. The proposed filter was based on a WLR with four different resonant frequencies: 1.23 GHz, 2.49 GHz, 3.73 GHz, and 5.41 GHz. By carefully selecting the resonant frequencies of the two resonators to be slightly different, the phase difference for the signals in the two resonators was negative, indicating that energy cancellation occurred, resulting in wide bandwidths and deep transmission zeros. The spurious resonant frequencies of the SIR were designed to be non-integer multiples of the fundamental resonant frequency by adjusting the length, characteristic impedance ratio, and electrical length. The SIR was designed to have three resonant frequencies at around 2.27 GHz, 3.37 GHz, and 4.94 GHz, which had phase differences with the WLR's resonant frequencies of 2.49 GHz, 3.73 GHz, and 5.41 GHz. Finally, a novel quad-band filter with a narrow band in the L2-band (GPS, 1.227 GHz)

and three wide bands in the WIMAX (3.5 GHz) and WLAN (2.4 GHz and 5.2 GHz) was achieved.

1. INTRODUCTION

Multi-band bandpass filters with wide bandwidth, high selectivity, and small insertion loss have recently become essential requirements for next-generation wireless communication systems [1–8]. In the past, the basic method for designing multi-band bandpass filters consisted of using several resonators that were responsible for each resonant band. However, this method not only increased the device volume but also required additional matching circuits. So far, only a few studies have proposed designs for applications of triple- and quad-band filters. Lin designed a tri-band bandpass filter using $\lambda/4$ and stub-loaded resonators [9]. Chen et al. used three pairs of hairpin resonators to cascade the SIR input/output for a triple-band application [10]. Goudos et al. designed a triple-band bandpass filter by combining three pairs of open-loop rectangular ring resonators between two transmission lines [11]. Cheng and Yang developed a complex quad-band bandpass filter with good filtering properties by combining four different structure resonators [12]. Although these fabricated filters were well designed, investigation into novel multi-band bandpass filters is still required to enhance their performance.

This paper presents a novel method for designing a microstrip quad-band bandpass filter. An Al_2O_3 ceramic substrate ($\varepsilon_r = 9.4$) is used for pattern minimization because its dielectric constant is higher than that of an FR4 substrate. The proposed filter is based on a winding line-shaped resonator (WLR) with four resonant frequencies of 1.23 GHz, 2.49 GHz, 3.73 GHz, and 5.41 GHz. If the phase differences for the signals in different resonators are negative and coupled with microstrip lines, energy cancelation will occur [13, 14]. If we carefully design two resonators to have only a slight difference in their resonant frequencies, and the phase difference for the signals in the two resonators is negative, energy cancelation will happen, causing wide bandwidths and deep transmission zeros [15]. The spurious resonant frequencies of a stepped impedance resonator (SIR) can be designed to have non-integer multiples of the fundamental frequency. This characteristic can be used to control or suppress the spurious responses and shift the resonant frequencies of multi-passbands [16]. To achieve that, we designed a SIR that was positioned in parallel with the input/output microstrip lines to resonate at 2.27 GHz, 3.37 GHz, and 4.94 GHz. This method can be used to increase bandwidths and generate deep transmission zeros in the out-of-band rejections. In

this study, phase differences between the WLR and SIR were created at around 2.4 GHz, 3.5 GHz, and 5.2 GHz. A novel quad-band filter with a narrow band in the L2-band (GPS, 1.227 GHz) and three wide bands in the WIMAX (3.5 GHz) and WLAN (2.4 GHz and 5.2 GHz) was achieved.

2. THEOREM TO INCREASE BANDWIDTHS AND GENERATE DEEP TRANSMISSION ZEROS

To begin, the initial pattern shown in Figure 1, based on a $1/2\lambda_g$ open-loop rectangular ring resonator (Resonator L, the dotted section) and with dual-band bandpass characteristics, was used to demonstrate the design principle of this work. According to the dielectric constant of Al$_2$O$_3$ ceramic ($\varepsilon_r = 9.4$), the approximate length of the fundamental guided wavelength was calculated using Eq. (1) [17]:

$$V = \frac{C}{\sqrt{\varepsilon_r}} = f\lambda_g \tag{1}$$
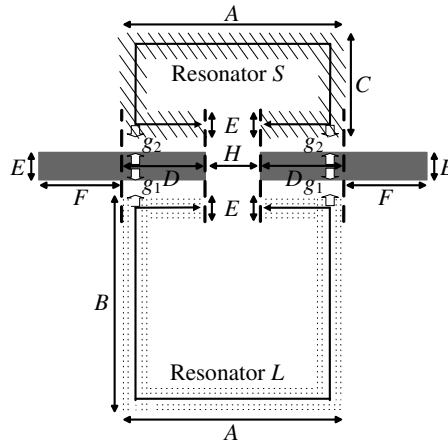
Figure 1. The proposed dual-band bandpass filter designed on an Al$_2$O$_3$ ceramic substrate.

As the fundamental resonant frequency was set at 1.23 GHz, the ideal microstrip line length of the approximate fundamental guided wavelength for a 1.23 GHz $1/2\lambda_g$ open-loop resonator was 39.78 mm (Resonator L). From the simulated results, the optimal coupling parameters between the input/output microstrip lines and the resonators were a gap of 0.1 mm and a length of 4 mm. As
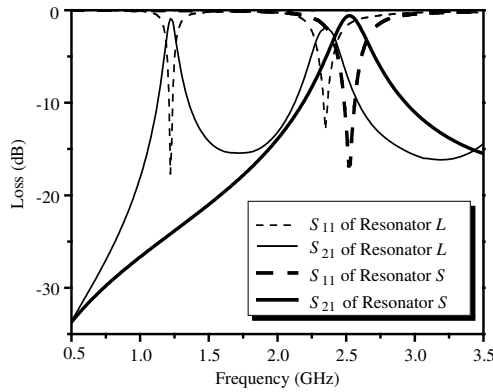
Figure 2. Simulated frequency responses of two different resonators.

Figure 2 shows, the first spurious resonance was close to 2.31 GHz and was a $1\lambda_g$ resonance, its value being about two times that of the $1/2\lambda_g$ fundamental resonance. However, even though the bandwidth of the 1.23 GHz band was adequate for the GPS-L2 band protocol, the bandwidth of the 2.31 GHz band was inadequate for 2.4 GHz WLAN application. To improve the bandwidth of the 2.4 GHz band alone, another resonator resonating close to 2.4 GHz was needed. As Figure 1 shows, a shorter open-loop rectangular ring resonator (Resonator S, the obliquely lined section) was positioned in parallel on the other side of the input/output microstrip lines, with the same coupling parameters as Resonator L. Resonator S was designed for 2.52 GHz and had a total length of 22 mm. The simulated resonant property of Resonator S is shown in Figure 2.

According to the literature [13–15], if the phase difference for signals in two paths is equal to 180°, energy cancelation occurs and no passband can be formed. With suitable tuning, two resonators with a slight difference in their resonant frequencies will operate at even and odd resonances, respectively, generating the change in phase required to implement a transmission zero. This method will enhance the bandwidths and generate the deep transmission zeros of the filter [12–14]. In the present structure, the 2.4 GHz band's bandwidth for the designed filter was enhanced by adjusting the length of Resonator S. Because a 180° phase difference around 2.4 GHz existed between Resonator L and Resonator S, the bandwidth of the second passband could be individually increased.

The voltage phase diagrams of the two resonators at two resonant frequencies are shown in Figure 3. The bandwidth of the 1.23 GHz band was generated by the $\lambda_g/2$ fundamental response of Resonator

L. The bandwidth of the 2.4 GHz band was generated by combining the $1\lambda_g$ first spurious response of Resonator L and the $\lambda_g/2$ fundamental response of Resonator S. A structure with a 180° phase difference was designed to achieve a deep transmission zero and a wider bandwidth for the 2.4 GHz band.

In the past, there were two methods to control the bandwidth of a microwave filter [12, 13]. In the first method, the bandwidth of each operating band increased as the coupling gap decreased, but the insertion losses also increased slightly. The second way to change the bandwidths was to shift the resonant frequencies of the resonators. Figure 4 shows the proposed dual-band bandpass filter with different C values; it is clear that the bandwidth of the 1.23 GHz band was almost unchanged. The bandwidth of the 2.4 GHz band increased with increasing C value because the length of C increased the fundamental resonant frequency of Resonator S. By carefully controlling the design parameters, the desired filter properties could be obtained.
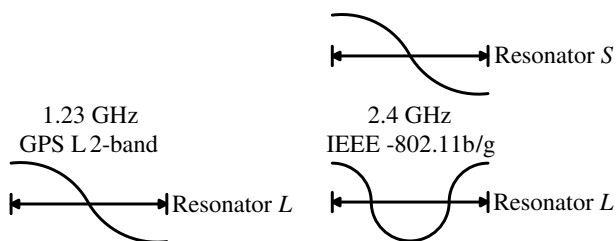
Figure 3. Voltage phase diagrams of two resonators.
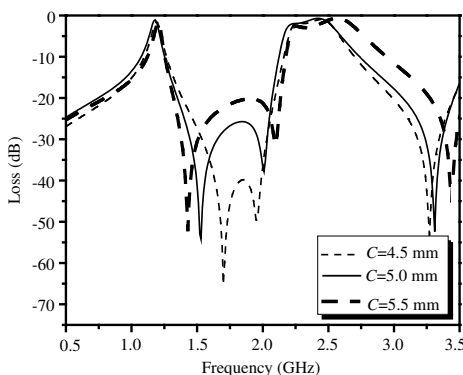
Figure 4. Properties of the proposed dual-band bandpass filter with different C values.

3. DESIGN PROCEDURES FOR THE QUAD-BAND BANDPASS FILTER

In this study, we propose a new structure according to the principles described above, combining a SIR and WLR to design a novel quad-band bandpass filter for application in different communication protocols. First, the proposed filter was based on a $1/2\lambda_g$ open-loop microstrip coupling line resonator and 1.23 GHz was selected as the fundamental resonant frequency of the open-loop resonator for the GPS L2-band. According to Eq. (1) and our simulation, the real length of the approximate fundamental guided wavelength in a straight line for the 1.23 GHz $1/2\ \lambda_g$ open-loop resonator was 42.0 mm. However, the device was too long for real use. To decrease the device length, the microstrip coupling line structure was changed to a WLR structure, as Figure 5 shows (dotted portion). The transmission lines were designed to be 1 mm wide to match the 50 Ω impedance. The coupling lengths and gap widths between the input/output transmission lines and the resonators were 7 mm (F) and 0.1 mm (g) and the optimal parameters of Y and N were 16 mm and 9 mm. The basic four resonant frequencies generated by the WLR structure were 1.23 GHz, 2.49 GHz, 3.73 GHz, and 5.41 GHz, as Figure 6 shows. Aside from the GPS L2-band, the quad-band
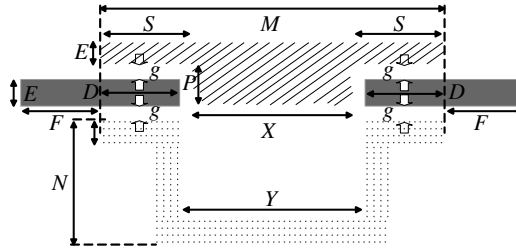
Figure 5. Proposed quad-band bandpass filter with two different resonators positioned in parallel (dotted area: WLR; obliquely lined area: SIR).

bandpass filter was also designed for WIMAX (3.5 GHz) and WLAN (2.4 GHz and 5.2 GHz). However, as Figure 6 shows, the narrow bandwidths and small out-of-band rejections were inadequate for real use. To improve the bandwidths of the 2.4 GHz, 3.5 GHz, and 5.2 GHz bands, the resonator had to have multi-resonant frequencies and spurious responses that were non-integer multiples of the fundamental resonant frequency. The traditional multiband bandpass filters were cascaded using several resonators with the same parameters, and it
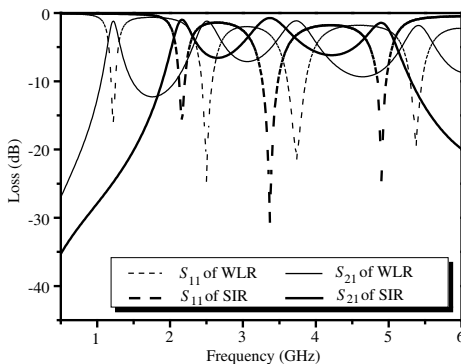
Figure 6. Simulated responses of designed WLR and SIR.

Figure 7. Typical stepped impedance resonator.

was difficult to asymmetrically adjust their respective operating bands, as we knew that a SIR could generate spurious frequencies in non-integer multiples of the fundamental resonant frequency by changing its characteristic impedance ratio (k) and electrical length (θ), as Figure 7 shows. In general, $\theta_1 = \theta_2 = \theta_0$ were selected and the relevant resonant frequencies, f_0, f_{s1}, and f_{s2} were determined [10, 16, 17]:

$$k = \frac{Z_2}{Z_1} \tag{2}$$

$$\alpha = \frac{2\theta_2}{2\theta_2 + 1\theta_1} = \frac{\theta_2}{\theta_0} \tag{3}$$

$$\tan^2 \theta_0 = k \tag{4}$$

$$\frac{f_{s1}}{f_0} = \frac{\theta_{s1}}{\theta_0} = \frac{\pi}{2 \tan^{-1} \sqrt{k}} \tag{5}$$

$$\frac{f_{s2}}{f_0} = \frac{\theta_{s2}}{\theta_0} = 2\left(\frac{f_{s1}}{f_0}\right) - 1 \tag{6}$$

The ratios of $3.5\,\text{GHz}$ to $2.4\,\text{GHz}$ and of $5.2\,\text{GHz}$ to $2.4\,\text{GHz}$ were approximately 1.46 and 2.17, respectively. To design the prototype SIR, values of $k = 3$ and $\alpha = 0.57$ were initially selected. After

optimal tuning, the parameters of the designed SIR in Figure 5 (obliquely lined part) were $X = 12 \, \text{mm}$, $S = 8 \, \text{mm}$, $M = 28 \, \text{mm}$, and $P = 4.5 \, \text{mm}$. By finely adjusting the frequencies of the two resonators, energy cancellation, and therefore a transmission zero, occurred in the proximity of the center frequency, leading to sharp selectivity between the passbands and the out-of-bands [12–14]. Thus, this method was used to enhance the bandwidths and achieve deep transmission zeros for the 2.4 GHz, 3.5 GHz, and 5.2 GHz bands.

According to Figure 4 and references [13, 14], the bandwidths of the two poles' operating bands were decided by the splitting of two modes in each band (besides the 1.23 GHz band). Figure 8 shows the resonant frequencies of the two resonators. According to SIR theory and Eqs. (1)–(6), the fundamental mode (the first resonant mode) at around the 2.4 GHz band, the first spurious resonant frequency (the second resonant mode) at around the 3.5 GHz band, and the second spurious resonant mode (the third resonant mode) at around the 5.2 GHz band of the SIR were obtained by tuning the SIR's total length (M), characteristic impedance ratio (k), and electrical length (θ). This was an important factor for controlling the modes of the two different resonators in each band. When these two modes were too close, the filter showed a narrow passband. When the two modes were far away, they created a serious ripple effect in the passband. By careful tuning of the SIR impedance parameters, the proposed quad-band bandpass filter presents wide bandwidth and small ripples in the passbands, as well as deep transmission zeros in the out-of-band rejections. Obviously, this structure has a major advantage in that the two resonators have very small interactions with each other, so each
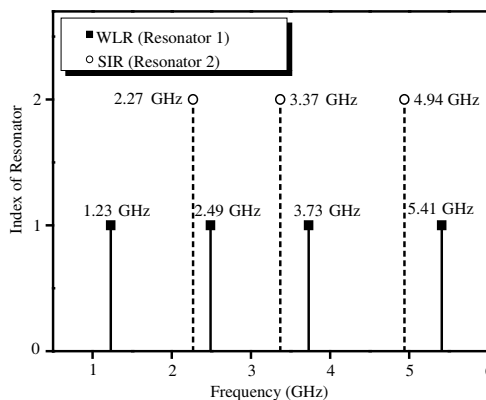
Figure 8. Resonant frequencies of two resonators.

one can be optimized separately, then they can be combined to form the final structure with minimal tuning.

4. EXPERIMENTAL PROCESS

Although Rogers Duroid boards offer a higher dielectric constant of 10.2 and a small dielectric loss of 0.0035, they are too expensive for popular commercial applications. Al_2O_3 ceramic substrates 1 mm thick have a comparably high dielectric constant ($\varepsilon_r = 9.4$), low dielectric loss (less than 0.001), and low price. For those reasons, Al_2O_3 ceramic substrates were chosen not only for pattern minimization but also for easy integration with the other RF circuits. A printing method involving low environmental pollution was used to fabricate the proposed quad-band bandpass filter, as the printing method did not require $FeCl_3$ solution to etch the Cu plate from the surfaces of the Duroid or FR4 substrates [17, 18]. After the optimal parameters for the designed quad-band bandpass filter were found, a printing mask was created according to the designed patterns and used to print the Ag/Pd paste on the Al_2O_3 ceramic substrate. The printed pattern was sintered at 700°C for 15 min. Two SMA connectors were welded to be the input/output. Finally, the microwave properties were measured using an Agilent-N5230A network analyzer.

5. RESULTS AND DISCUSSION

Figure 9 illustrates the resonant current distributions in the WLR structure of the proposed quad-band filter. The fundamental, first spurious, second spurious, and third spurious modes are sketched according to the simulated results from Ansoft HFSS. As Figure 9(a) shows, two zero points appeared at the front/end edges and the maximum current appeared in the middle of the resonator. This means that the length of the WLR structure was equal to the half guided wavelength fundamental response for 1.23 GHz. Figure 9(b) shows three zero points at the front/end edges and the middle of the resonator, and two maximum current density zones distributed between those zero points. This means that the length of the WLR structure is equal to the full guided wavelength spurious response at 2.49 GHz. Similarly, Figure 9(c) and Figure 9(d) show four and five zeros and reveal 3/2 λ_g and 2 λ_g spurious responses at 3.73 GHz and 5.41 GHz, respectively.

     Figure 10 shows the different resonant current distributions in the SIR of the proposed filter. The current distribution in Figure 10(a) was atypical, as it included one primary current density zone and
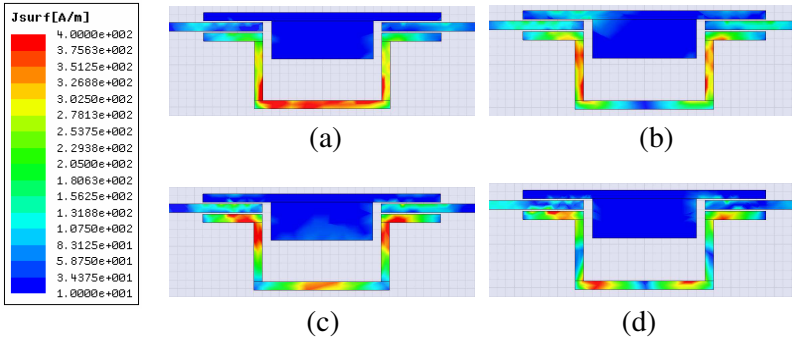
Figure 9. Simulated resonant current distribution of WLR for (a) fundamental resonant at 1.23 GHz, (b) first spurious resonant at 2.49 GHz, (c) second spurious resonant at 3.73 GHz, and (d) third spurious resonant at 5.41 GHz.
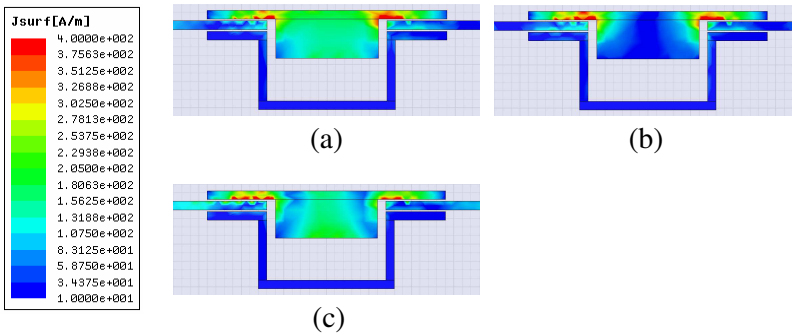
Figure 10. Simulated resonant current distribution of SIR for (a) fundamental resonant at 2.27 GHz, (b) first spurious resonant at 3.37 GHz, and (c) second spurious resonant at 4.94 GHz.

one secondary current density zone. This was the mode between resonant paths $1/2\ \lambda_g$ and $1\ \lambda_g$, which was inferred to be resonant path $2/3\ \lambda_g$. Because three and four zero points were present, the current distributions in Figure 10(b) and Figure 10(c) indicate spurious responses $1\lambda_g$ and $3/2\lambda_g$ at 3.37 GHz and 4.94 GHz. Even in the same resonant path, $3/2\ \lambda_g$, shown in Figure 10(c), the maximum current density zone of the SIR in the middle section was weaker than the other two maximum current density zones. This is because the low impedance region was wider than the high impedance region.

In the proposed quad-band filter, the 1.23 GHz GPS L2-band was formed using the fundamental response of the WLR. The 2.4 GHz

WLAN was formed by combining the first spurious response of the WLR with the fundamental response of the SIR. The 3.5 GHz WIMAX was formed by combining the second spurious response of the WLR with the first spurious response of the SIR. Finally, the 5.2 GHz WLAN was formed by combining the third spurious response of the WLR with the second spurious response of the SIR. Comparing the results in Figures 9(b), (c), and (d) with those in Figures 10(a), (b), and (c), the resonant phases of the two resonators at the 2.4 GHz band, 3.5 GHz band, and 5.2 GHz band are quite different, and are similar to the functions of even mode and odd mode resonances. If the resonant frequencies of both modes had been entirely the same in each band, the interactions of the signals in both paths would have led to energy cancellation, and no passbands would have appeared. However, adjusting the frequencies of the two modes to be slightly different in each band achieved a wide passband with deep transmission zeros in the out-of-band. This design effectively increased the high signal selectivity between passbands and out-of-bands. Figure 11 shows a photograph of the fabricated quad-band bandpass filter, which has a compact size of 36 mm × 11.4 mm (without the SMA).
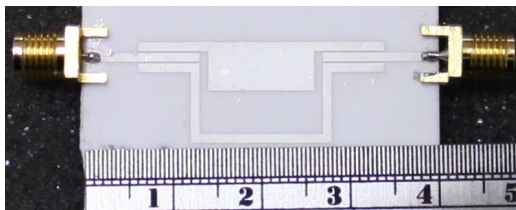
Figure 11. Photograph of the fabricated filter.

Figure 12 compares the simulated and measured properties of the proposed filter. The measured group delay has the typical results, the positive peaks present at the resonant frequencies of S_{11} peaks and the negative peaks present at those of transmission zeros. The simulated frequency responses are $S_{21} = 1.49$ dB and $BW = 70$ MHz (5.69%) at 1.23 GHz, $S_{21} = 0.98$ dB and $BW = 410$ MHz (16.73%) at 2.45 GHz, $S_{21} = 1.27$ dB and $BW = 680$ MHz (19.21%) at 3.54 GHz, and $S_{21} = 1.76$ dB and $BW = 550$ MHz (10.61%) at 5.19 GHz. The measured frequency responses are $S_{21} = 1.79$ dB and $BW = 60$ MHz (4.92%) at 1.22 GHz, $S_{21} = 1.76$ dB and $BW = 390$ MHz (16.39%) at 2.38 GHz, $S_{21} = 1.85$ dB and $BW = 790$ MHz (21.76%) at 3.63 GHz, and $S_{21} = 2.27$ dB and $BW = 680$ MHz (13.03%) at 5.22 GHz. The simulated transmission zeros are 45.53 dB at 1.76 GHz, 30.21 dB at 2.79 GHz, and 38.85 dB at 4.23 GHz. The measured transmission
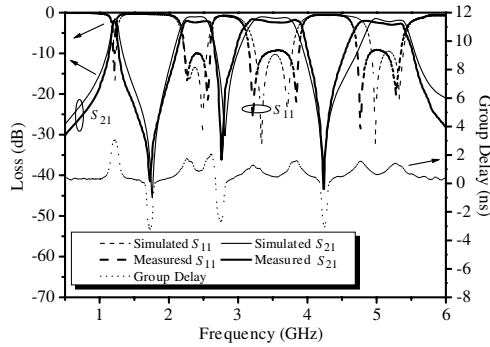
Figure 12. Simulated and measured results for the proposed filter.

zeros are 41.51 dB at 1.73 GHz, 36.17 dB at 2.76 GHz, and 43.36 dB at 4.23 GHz. The bandwidths of the fabricated filter for GPS-L2 band (1.227 GHz, narrow band), WiMAX band (3.4 GHz $\sim$ 3.8 GHz), and WLAN bands (2.4 GHz $\sim$ 2.4835 GHz and 5.15 GHz $\sim$ 5.35 GHz) are 60 MHz (1.20 GHz $\sim$ 1.26 GHz), 790 MHz (3.12 GHz $\sim$ 3.91 GHz), and 390 MHz (2.20 GHz $\sim$2.59 GHz) and 680 MHz (4.73 GHz $\sim$ 5.41 GHz), respectively. It is clear that the bandwidths of the fabricated filter have covered the communication protocols of the four required passbands. As the measured results show, the insertion loss of the measured results is little larger than that of the simulated results because of the additional loss caused by welded imperfection. The ripple is observed in the passbands because of the increases of modes splitting caused by fabricated imperfections. From inspection of Figure 12, it can be seen that the measured results agree well with the simulated results and the proposed filter is suitable for GPS-L2, WiMAX, and WLAN quad-band applications.

6. CONCLUSIONS

This study presents a novel microstrip quad-band bandpass filter by combining two different resonators, WLR and SIR, positioned in parallel along the two sides of the input/output transmission lines. The WLR and SIR resonators operated similarly with even and odd resonances, respectively, and generated the change in phase required to implement transmission zeros between two resonators at the 2.4 GHz band, 3.5 GHz band, and 5.2 GHz band. In addition, this structure has the major advantage that the two resonators have very small interactions with each other, so each one can be optimized separately, and then the two can be combined to form the final structure with very little tuning. The proposed filter has one adequate bandwidth for

GPS-L2 and three wide bands for WiMAX and WLAN, plus three deep transmission zeros among the four passbands for signal selectivity. It also has the advantages of simple circuit, tiny size, easy fabrication, and low environmental pollution, making it suitable for GPS-L2, WiMAX, and WLAN quad-band applications.

ACKNOWLEDGMENT

REFERENCES

1. Yang, G. M., R. Jin, C. Vittoria, V. G. Harris, and N. X. Sun, "Small ultra-wideband (UWB) bandpass filter with notch band," *IEEE Microwave Wireless Compoents Letters*, Vol. 18, No. 3, 176–178, 2008.

2. Zhou, Y. and S. Lucyszyn, "Modelling of reconfigurable terahertz integrated architecture (Retina) SIW structures," *Progress In Electromagnetics Research*, Vol. 105, 71–92, 2010.

3. Yin, Q., L.-S. Wu, L. Zhou, and W.-Y. Yin, "Compact dual-band bandpass filter using asymmetrical dual stub-loaded open-loops," *Journal of Electromagnetic Waves and Applications*, Vol. 24, Nos. 17–18, 2397–2406, 2010.

4. Chen, C.-Y. and C.-C. Lin, "The design and fabrication of a highly compact microstrip dual-band bandpass filter," *Progress In Electromagnetics Research*, Vol. 112, 299–307, 2011.

5. Wen, S. and L. Zhu, "Numerical synthesis design of coupled resonator filters," *Progress In Electromagnetics Research*, Vol. 92, 333–346, 2009.

6. Hu, G., C. Liu, L. Yan, K. Huang, and W. Menzel, "Novel dual mode substrate integrated waveguide band-pass filters," *Journal of Electromagnetic Waves and Applications*, Vol. 24, Nos. 11–12, 1661–1672, 2010.

7. Mo, S.-G., Z.-Y. Yu, and L. Zhang, "Design of triple-mode bandpass filter using improved hexagonal loop resonator," *Progress In Electromagnetics Research*, Vol. 96, 117–125, 2009.

8. Chen, W.-N. and W.-K. Chia, "A novel approach realizing 2.4/5.2 GHz dual-band BPFs using twin-spiral etched ground structure," *Journal of Electromagnetic Waves and Applications*, Vol. 23, No. 7, 829–840, 2009.

9. Lin, X.-M., "Design of compact tri-band bandpass filter using $\lambda/4$ and stub-loaded resonators," *Journal of Electromagnetic Waves and Applications*, Vol. 24, Nos. 14–15, 2029–2035, 2010.

10. Chen, C. F., T. Y. Huang, and R. B. Wu, "Design of dual- and triple-passband filters using alternately cascaded multiband resonators," *IEEE Trans. Microw. Theory Tech.*, Vol. 54, No. 9, 3550–3558, 2006.

11. Goudos, S. K., Z. D. Zaharis, and T. Yioultsis, "Application of a differential evolution algorithm with strategy adaptation to the design of multi-band microwave filters for wireless communications," *Progress In Electromagnetics Research*, Vol. 109, 123–137, 2010.

12. Cheng, C. M. and C. F. Yang, "Develop quad-band (1.57/2.45/3.5/5.2 GHz) bandpass filters on the ceramic substrate," *IEEE Microwave Wireless Components Letters*, Vol. 20, No. 5, 268–270, 2010.

13. Rosenberg, U. and S. Amari, "Novel coupling schemes for microwave resonator filters," *IEEE Trans. Microwave Theory Tech*, Vol. 50, 2896–2902, Dec. 2002.

14. Rebenaque, D. C., F. Q. Pereira, J. P. García, A. A. Melcón, and M. Guglielmi, "Two compact configurations for implementing transmission zeros in microstrip filters," *IEEE Microwave Wireless Components Letters*, Vol. 14, No. 10, 475–477, 2004.

15. Osipenkov, V. and S. G. Vesnin, "Microwave filters of parallel cascade structure," *IEEE Trans. Microwave Theory Tech.*, Vol. 42, 1360–1367, 1994.

16. Makimoto, M. and S. Yamashita, "Bandpass filters using parallel coupled stripline stepped impedance resonators," *IEEE Trans. Microw. Theory Tech.*, Vol. 28, No. 12, 1413–1417, 1980.

17. Hong, J. S. and M. J. Lancaster, *Microstrip Filters for RF/Microwave Applications*, Wiley, New York, 2001.

18. Kung, C.-Y., Y.-C. Chen, S.-M. Wu, C.-F. Yang, and J.-S. Sun, "A novel compact 2.4/5.2 GHz dual wideband bandpass filter with deep transmission zero," *Journal of Electromagnetic Waves and Applications*, Vol. 25, Nos. 5–6, 617–628, 2011.

19. Yang, C. F., M. Cheung, C. Y. Huang, and J. S. Sun, "Print a compact single- and quad-band slot antenna on ceramic substrate," *Journal of Electromagnetic Waves and Applications*, Vol. 24, No. 13, 1697–1707, 2010.